JOC*Article*

Remote Position Substituents as Modulators of Conformational and Reactive Properties of Quinones. Relevance of the π/π Intramolecular Interaction

Guillermo Roura-Pérez,[†] Beatriz Quiróz,[†] Martha Aguilar-Martínez,[‡] Carlos Frontana,[§] Alejandro Solano,[‡] Ignacio González,[§] José Antonio Bautista-Martínez,[‡] Jesús Jiménez-Barbero,[¶] and Gabriel Cuevas*[,†]

Instituto de Química, Universidad Nacional Autónoma de México, Cd. Universitaria, Apdo. Postal 70213, 04510, México, D. F. México, Facultad de Química, Universidad Nacional Autónoma de México, Circuito Escolar, Cd. Universitaria, 04510, México, D. F. México, Universidad Autónoma Metropolitana-Iztapalapa, Departamento de Química, Apdo. Postal 55-534, 09340 México, D. F. México, and Centro de Investigaciones Biológicas, Consejo Superior de Investigaciones Científicas, c/Ramiro Maetzu 9, 28040 Madrid, Spain

gecgb@servidor.unam.mx

Received July 30, 2006

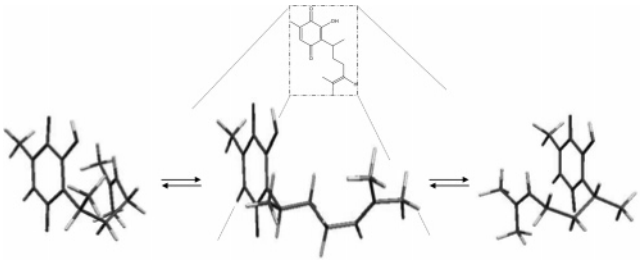

Several studies have described that quinoid rings with electron-rich olefins at remote position experience changes in their redox potential. Since the original description of these changes, different approaches have been developed to describe the properties of the binding sites of ubiquinones. The origin of this phenomenon has been attributed to lateral chain flexibility and its effect on the recognition between proteins and substrates associated with their important biological activity. The use of electrochemical−electron spin resonance (EC−ESR) assays and theoretical calculations at MP2/6-31G(d,p) and MP2/6-31++G(d,p)//MP2/6-31G(d,p) levels of several conformers of perezone [(2-(1,5-dimethyl-4-hexenyl)-3-hydroxy-5-methyl-1,4-benzoquinone] established that a weak $\pi-\pi$ interaction controls not only the molecular conformation but also its diffusion coefficient and electrochemical properties. An analogous interaction can be suggested as the origin of similar properties of ubiquinone Q_{10}. The use of nuclear magnetic resonance rendered, for the first time, direct evidence of the participation of different perezone conformers in solution and explained the cycloaddition process observed when the aforementioned quinone is heated to form pipitzols, sesquiterpenes with a cedrene skeleton. The fact that biological systems can modulate the redox potential of this type of quinones depending on the conformer recognized by an enzyme during a biological transformation is of great relevance.

Introduction

Electron-transfer processes are a fundamental part of life because they participate in many metabolic reactions where energy conservation is essential.[1−4] A group of natural products known as quinones plays an important role in these types of reactions, particularly in redox processes such as mitochondrial respiration[5] and photosynthesis.[6] Since quinones actively participate in electron-transfer processes, the study of their structural properties is important.[7] It is well-known that a modification

[†] Instituto de Química, Universidad Nacional Autónoma de México.
[‡] Facultad de Química, Universidad Nacional Autónoma de México.
[§] Universidad Autónoma Metropolitana-Iztapalapa.
[¶] Consejo Superior de Investigaciones Científicas.

(1) Stryer, L. *Biochemistry*, 4th ed.; Stanford University: Stanford, CA, 1995; Chapter 21, p 529 and Chapter 26, p 653.

(2) Berlin Y. A.; Kurnikov, I. V.; Beratan, D.; Ratner, M. A.; Burin, A. L. In *DNA Electron Transfer Processes: Some Theoretical Notions*; Schuster, G. B., Ed.; Springer: New York, 2004.

(3) Isied, S. S. Mediation of Electron Transfer by Peptides and Proteins. Current Status. In *Metal Ions in Biological Systems*: *Electron Transfer Reactions in Metalloproteins*; Sigel, H., Ed.; Marcel Dekker: New York, 1991; Vol. 27, Chapter 1, pp 1−56.

(4) Lanz, G. *FEBS Lett.* **2001**, *509*, 151.

10.1021/jo061576v CCC: $37.00
Published on Web 02/15/2007

SCHEME 1. Some Relevant Quinones Substituted by Unsaturated Groups

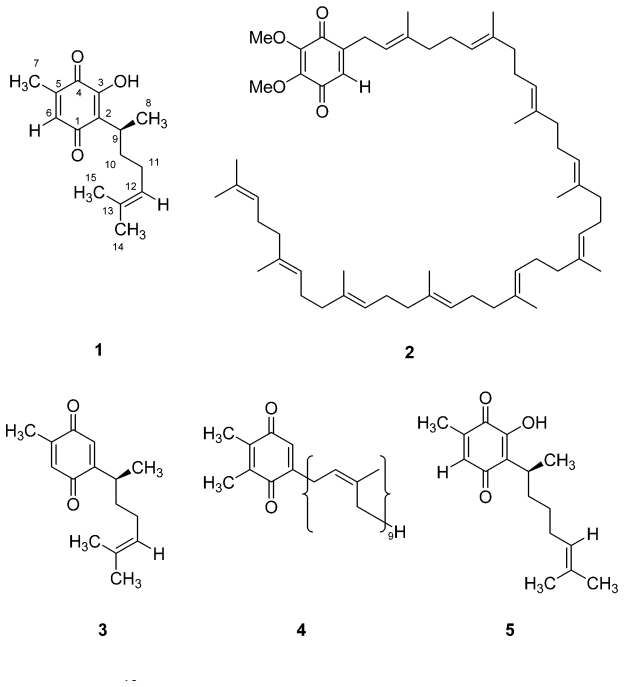

in the direct substitution pattern on the quinoid ring impacts its capability to accept electrons[8] and, thus, its capacity to mediate biological reactions. There are several naturally occurring quinones substituted with aliphatic groups with double bonds at remote positions. Examples of these compounds include perezone (**1**, Scheme 1),[9] ubiquinones that contain a prenyl moiety with 5 (Q_1) to 50 carbon atoms (Q_{10})[10] (**2**), curcuquinone (**3**),[11] and polyprenyl quinones (**4**). Even though these molecules are very important in biological processes, the substituent at a remote position and its potential participation in these processes have received little attention.

Yu et al.[12] have studied the effect of the side chain of ubiquinone and some of its derivatives on their capacity to transfer electrons. The authors reported that the electron acceptor capability is maximum when the chain has at least six carbon atoms and decreases with the addition of unsaturations. These authors also described that chain flexibility is important for electron transfer involved in electrochemical activity and protein recognition involved in redox process mediation. However, it is still not clear if the lateral chain length and flexibility are the only key factors involved in the redox activity of the molecule. Therefore, the determination of the origin of this effect as well as its possible implications in supramolecular chemistry was considered important. The understanding of this phenomenon is of key interest because the description of the intramolecular interaction could be extrapolated to intermolecular cases. In addition, other authors propose that a branched chain with a methyl group and the rest of the isoprene unit that includes a double bond (C═C) are responsible for the increased affinity of ubiquinone Q_2 for the binding site.[13] Recently, this information was confirmed when it was reported that the substrates that show an optimum affinity for the receptor have a chain of 10 carbon atoms.[14] When the elevated diffusion coefficient of ubiquinone Q_{10} and calculations using both molecular dynamics[15] and semiempirical methods (PM3)[16] are considered, it can be proposed that the molecule should adopt a folded conformation. This can be further confirmed by studies using EPR, ENDOR, and TRIPLE resonance[17] that allow the analysis of radical anions and cations of Q_0, Q_6, and Q_{10}. In fact, quinone's electrochemical properties have been used for the development of analytical methods for the detection of coenzyme Q_{10}. These methods are based on the measurement of the intermediary radical (semiquinone) formed during the reduction of Q_{10} using in situ EPR spectroelectrochemical techniques.[18] However, the study of the described coupling constants reported in several papers cited herein[16,17] does not help in establishing the proximity between the substituent at remote position and the quinone. These studies have triggered the interest in both the determination of the precise site for molecular recognition of diverse cytochromes and the synthesis of analogous compounds with inhibitory properties.[19−23]

Noncovalent interactions are at the heart of supramolecular chemistry.[24] Hydrogen bonds are perhaps the better known and most studied of the forces involved in molecular recognition studies.[24] However, it has been shown that other interactions, weaker in nature, such as CH/π and π/π, may also be responsible for a variety of molecular recognition phenomena.[25,26] The understanding of π/π interactions has become a topic of interest, and important progress has been made in the construction of complex ensembles, that is, by applying these interactions to self-assembly processes. The study of these interactions has been generally conducted employing well-defined conformational arrangements in the solid state. Despite the importance of this methodology, the prediction of the complete control of conformational processes and molecular reactivity is limited with this approach. The evaluation of the strength of π/π interactions as well as the identification of

(5) Crane, F. L. *Annu. Rev. Biochem.* **1977**, *46*, 439.
(6) (a) Bentley, R.; Campbell, I. M. In *The Chemistry of Quinoid Compounds*; Patai, S. Ed.; John Wiley & Sons: London, 1974; pp 683−736. (b) Nohl, H.; Jordan, W.; Youngman, R. J. *Adv. Free Radical Biol. Med.* **1986**, *2*, 211.
(7) Lenaz, G. *Biochim. Biophys. Acta* **1998**, *1364*, 207.
(8) Aguilar-Martínez, J. A.; Cuevas, G.; Jiménez-Estrada, M.; González, I.; Lotina-Hennsen, B.; Macías-Ruvalcaba, N. *J. Org. Chem.* **1999**, *64*, 3684.
(9) Joseph-Nathan, P. *Rev. Soc. Quim. Mex.* **1974**, *18*, 226.
(10) Yu, C. A.; Yu, L. *Biochemistry* **1982**, *21*, 4096.
(11) Yoshimura, T.; Kisyuku, H.; Kamei, T.; Takabatake, K.; Shindo, M.; Shishido, K. *ARKIVOC* **2003**, *8*, 247.
(12) Yu, C.; Lianquan, G.; Lin, Y.; Yu, L. *Biochemistry* **1985**, *24*, 3897.
(13) Sakamoto, K.; Miyoshi, H.; Ohshima, M.; Kuwabara, K.; Kano, K.; Akagi, T.; Mogi, T.; Iwamura, H. *Biochemistry* **1998**, *37*, 15106.
(14) Simkovic, M.; Frerman, F. E. *Biochem. J.* **2004**, *378*, 633.
(15) Di Bernanrdo, S.; Fato, R.; Casadio, R.; Fariselli, P.; Lenaz, G. *FEBS Lett.* **1988**, *426*, 77.
(16) Joela, H.; Kasa, S.; Lehtovuori, P.; Bech, M. *Acta Chem. Scand.* **1997**, *51*, 322.
(17) Lehtovuori, P.; Joela, H. *J. Magn. Reson.* **2000**, *145*, 319.
(18) Long, Y. T.; Yu, Z. H.; Chen, H. Y. *Electrochem. Commun.* **1999**, *1*, 194.
(19) Zhang, L.; Li, Z.; Quinn, B.; Yu, L.; Yu, C.-A. *Biochim. Biophys. Acta* **2002**, *1556*, 226.
(20) Oyedotum, K. S.; Lemiere, B. D. *J. Biol. Chem.* **2001**, *276*, 16936.
(21) Ohshima, S.; Miyoshi, H.; Sakamoto, K.; Takegami, K.; Iwata, J.; Kuwabara, K. *Biochemistry* **1998**, *37*, 6436.
(22) Esposti, M. D.; Ngo, A.; McMullen, G. L.; Ghelli, A.; Sparla, F.; Benelli, B.; Ratta, M.; Linnane, A. W. *Biochem. J.* **1996**, *313*, 327.
(23) Tremblay, M. S.; Sames, D. *Org. Lett.* **2005**, *7*, 2417.
(24) Atwood, J. L., Steed, J. W., Eds. *Encyclopedia of Supramolecular Chemistry*; Marcel Dekker, Inc.: New York, 2004.
(25) Nishio, M. Weak Hydrogen Bonds. In *Encyclopedia of Supramolecular Chemistry*; Atwood, J. L., Steed, J. W., Eds.; Marcel Dekker, Inc.: New York, 2004; p 1576.
(26) Fernández-Alonso, M. C.; Cañada, J.; Jiménez-Barbero, J.; Cuevas, G. *J. Am. Chem. Soc.* **2005**, *127*, 7379 and references therein.

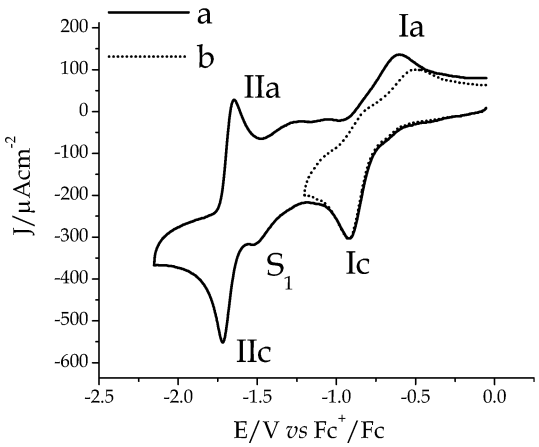

FIGURE 1. Typical cyclic voltammogram at different inversion potentials (E_λ) in the negative direction of 1 mM **1** in 0.1 M TFBTEA + acetonitrile. Glassy carbon as the working electrode. (a) $E_\lambda = -2.15$ V and (b) $E_\lambda = -1.21$ V. Potential scan rate = 0.1 V·s^{-1}.

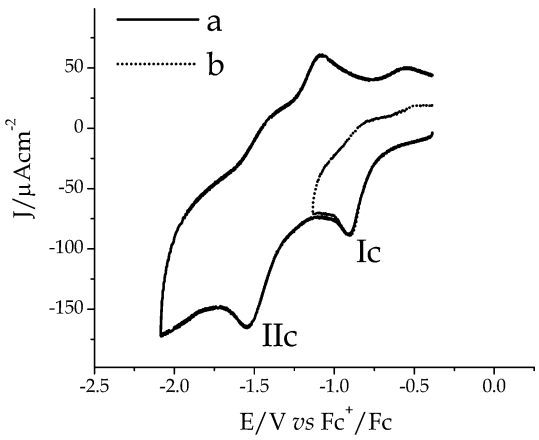

FIGURE 2. Typical cyclic voltammogram of 1 mM **1-H$_2$** in 0.1 M TFBTEA + acetonitrile. Glassy carbon as the working electrode. Potential scan rate = 0.1 V·s^{-1}. (a) $E_\lambda = -2.1$ V and (b) $E_\lambda = -1.135$ V.

possible π/π-controlled conformational processes is of particular interest because new avenues for the participation of these interactions in supramolecular processes could be opened. Information in this area will lead to better understanding of the design of supramolecular arrangements, thus providing the basis for crystal engineering and rational design of supramolecules. To date, according to Price, it has been intrinsically difficult to predict the crystallization patterns for a group of organic molecules because the determination of the crystal arrangements that a group of basically unknown organic molecules will adopt is indeed elusive.[27]

Perezone has been used to study the π/π interaction process between a rich electron olefin, as a remote position substituent, and the quinone ring. We have described the conformers that maintain the lateral chain and the quinoid ring of perezone in close proximity when found in solution. Their conformational preferences have also been studied to establish their origin and chemical consequences.

Results and Discussion

Perezone [2-(1,5-dimethyl-4-hexenyl)-3-hydroxy-5-methyl-1,4-benzoquinone,[9,28] **1**, Scheme 1] is a quinone with a double bond at remote position. This sesquiterpenic quinone was first isolated in 1850 from the roots of *Perezia cuernavacana*, a plant traditionally used in Mexico as an antiparasitic agent.[29] Perezone is an excellent model to study the π/π interaction between a donating olefin rich in electrons and a quinone group of captive nature basically because the distance between these groups is the shortest available that allows the interaction of interest. In fact, it is commonly accepted that the first unit of isoprene is responsible for the high affinity between ubiquinone and the reduction site.[13] The reduction of the olefin is very clean and yields a pure product without byproducts. In addition, its molecular size allows high-level calculations that include the dispersion terms that are fundamental for the correct description of the π/π interaction. The potential energy surface is simplified when numerous stationary states that generate long and flexible chains are eliminated. The results obtained using this model can be easily extrapolated to analogous systems such as ubiquinone Q_n.

SCHEME 2. Product of Hydrogenation of Perezone (1)

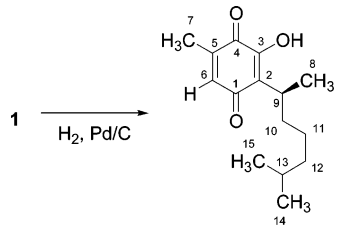

Perezone was isolated as golden-yellow leaflets, a crystalline solid[30,31] that, when hydrogenated using the procedure reported by Kölg and Boer,[32] generates product **1-H$_2$** with the C12−C13 double bond reduced (Scheme 2).

I. Electrochemistry of Perezone and Dihydroperezone (1 and 1-H$_2$). The electrochemical study of both molecules **1** and **1-H$_2$** was performed in order to evaluate their electron-transfer properties. Typical cyclic voltammograms for the reduction of perezone and its derivative **1-H$_2$** in acetonitrile are depicted in Figures 1 and 2, respectively. Perezone (**1**, Figure 1) presents two electron-transfer signals, the first (I_c) occurs at a cathodic peak potential (E_{pc}) of −0.926 V. When the potential scan was inverted at $E_\lambda = -1.21$ V (Figure 1b), an anodic signal appears at an anodic peak potential (E_{pa}). The $\Delta E_p = E_{pa} - E_{pc}$ value is above 0.3 V. Also the current density ratio j_{pa}/j_{pc} is smaller than 0.6. The high ΔE_p value observed for peak I_c suggests irreversibility in the system due to either chemical reactions

(27) Price, S. L. Crystal Structure Prediction. In *Encyclopedia of Supramolecular Chemistry*; Atwood, J. L., Steed, J. W., Eds.; Marcel Dekker, Inc.: New York, 2004; p 371.

(28) (a) Morton, R. A., Ed. *Biochemistry of Quinones*; Academic Press: New York, 1965. (b) Patai S., Rappoport, Z., Eds. *The Chemistry of Quinonoid Compounds*; Wiley and Sons: New York, 1988; Vol. II.

(29) Rio de la Loza, L. *Disertación Presentada a la Academia de Medicina*, 1852.

(30) Walls, F.; Salmón, M.; Padilla, J.; Joseph-Nathan, P.; Romo, J. *Bol. Inst. Quim. Univ. Nac. Auton. Mex.* **1965**, *17*, 3.

(31) Aguilar-Martínez, M.; Bautista-Martinez, J. A.; Macías-Ruvalcaba, N.; González, I.; Tovar, E.; Marín del Alizal, T.; Collera, O.; Cuevas, G. *J. Org. Chem.* **2001**, *66*, 8349.

(32) (a) Kögl, F.; Boer, A. G. *Recl. Trav. Chim.* **1935**, *54*, 779−784. (b) Archer, D. A.; Thomson R. H. *J. Chem. Soc. (C)* **1967**, 1710.

coupled with the electron transfer or kinetic complications.[33] The j_{pa}/j_{pc} ratio value and the dependency of E_{pc} as a function of the scan rate (υ, not shown) demonstrated the presence of chemical reactions coupled to the electron transfer. The second electro-reduction wave of **1** at −1.72 V (II_c) exhibits characteristics of a reversible electron transfer, with a ΔE_p value near 0.06 V and j_{pa}/j_{pc} equal to unity. Between peaks I_c and II_c, it is possible to observe the presence of an ill-defined shoulder (S_1), which is associated with the electro-reduction of a quinone homoconjugated species.[34−36]

The electrochemical behavior of **1** has been observed in the electro-reduction of other quinones containing internal proton donors,[37] such as an −OH group at the C3 position in **1** (represented as HQ in the reaction sequence 1−5). In these cases, the electro-reduction pathway has been described through a series of consecutive proton- and electron-transfer reactions.[38,39]

$$HQ + 1e^- \rightleftarrows HQ^{\bullet -} \quad (1)$$

$$HQ^{\bullet -} + HQ \rightleftarrows HQH^{\bullet} + Q^- \quad (2)$$

$$HQH^{\bullet} + 1e^- \rightleftarrows HQH^- \quad (3)$$

or

$$HQH^{\bullet} + HQH^{\bullet} \rightleftarrows HQ + HQH_2 \quad (3')$$

$$HQH^- + HQ \rightleftarrows HQH_2 + Q^- \quad (4)$$

$$3HQ + 2e^- \rightleftarrows HQH_2 + 2Q^- \quad (5)$$

From these reports, the first reduction peak of **1** (I_c) can be associated with the global reaction (eq 5) where three molecules of **1** require two electrons to produce only one hydroquinone molecule and two molecules of the conjugated base of **1** Q^-. This means that only one molecule of quinone is reduced (eqs 1 and 3) and two molecules are deprotonated (eqs 2 and 4). However, the amount of deprotonated quinone depends on the acidity of the −OH function at position C3. If this proton is not acidic enough to protonate the electrogenerated bases, the final reduction step would be interrupted on either reaction 3 or 4, and therefore the global stoichiometry would change. Under these conditions, the corresponding oxidation peak of the hydroquinone monoanion (HQH^-) would appear at an E_{pa} value closer to the first reduction peak. When the acidity of the −OH function increases, it allows the formation of the protonated hydroquinone derivative (HQH_2) which would be oxidized at a more positive potential in relation to the hydroquinone monoanion.[40,41]

The experimental case for **1** can be evaluated by analyzing the responses at different inversion potentials for signal I_c. When the potential scan was inverted at E_λ= −1.21 V (Figure 1b), the presence of peak I_a, located at −0.51 V, indicated that the electro-reduction process involved in wave I_c corresponds to the formation of the monoanion hydroquinone. Therefore, the global reaction corresponding to peak I_c goes through the following stoichiometry (eq 6).

$$2HQ + 2e^- \rightleftarrows HQH^- + Q^- \quad (6)$$

The intermediaries formed in the series of reactions (eqs 1−4) suggest that the second peak (II_c) belongs to the formation of the corresponding dianion radical ($Q^{\bullet 2-}$) through one-electron reduction of Q^- (eq 7)[37,41]

$$Q^- + e^- \rightleftarrows Q^{\bullet 2-} \quad (7)$$

Molecule **1-H$_2$** showed behavior in aprotic media similar to that described above for **1** (Figure 2). The first electro-reduction wave appeared as an irreversible electron transfer occurring at an E_{pc} value of −0.903 V. The difference between the E_{pc} values for the signals I_c for both compounds was small (0.023 V). This peak showed also a lower diffusion-controlled current, as compared to that corresponding to **1**. The differences in peak potential for signals I_c and I_a were higher than those for **1** (nearly 0.3 V). At the same time, it was found that the second electro-reduction signal, located at −1.58 V, lost the reversible behavior observed in **1**.

These results can be understood within the basis of the self-protonation reactions presented as eqs 1−5. From these reactions, it can be proposed that, for **1-H$_2$**, the reduction process is ruled by chemical eq 5. This global mechanism is compatible with the other responses analyzed since it would involve the formation of a protonated hydroquinone. This intermediate should be oxidized at more positive potential values,[40,41] as observed experimentally. Also, this mechanistic sequence involves a lower electron/quinone stoichiometry (by the differences in diffusion current), which is also presented by compound **1-H$_2$**. The difference in diffusion currents is not enough to be analyzed by a simple stoichiometry difference, as it is larger than expected (1 vs 2/3 between eqs 5 and 6; 1 vs 1/4 for the experimental case). Assuming that the same area and analytical concentrations for both compounds are occurring, the diffusion coefficient seems to be an option to explain the remaining difference. From the experimental responses, it can be proposed that the D value for **1** is higher than that for **1-H$_2$**. This result is indicative of a difference in the conformations for both compounds, which could be arising from the presence or absence of the double bond located at C12−C13.[12]

The influence of the double bond appears to be more significant for the second electron-transfer process, which corresponds to the formation of a radical dianion (eq 7), where the potential shift between the corresponding signal II_c for **1** and **1-H$_2$** is 0.14 V. This indicates that the analysis of the

(33) Bard, A. J.; Faulkner, L. R. *Electrochemical Methods: Fundamentals and Applications*, 2nd ed.; John Wiley and Sons: New York, 2001.
(34) Itho, S.; Kawakami, H.; Fukuzumi, S. *J. Am. Chem. Soc.* **1998**, *120*, 7271.
(35) Goulart, M. O. F.; Lima, N. M. F.; Santa'Ana, A. E. G.; Ferraz, P. A. L.; Cavalcanti, J. C. M.; Falkowski, P.; Ossowski, T.; Liwo, A. *J. Electroanal. Chem.* **2004**, *566*, 25.
(36) Salas, M.; Gómez, M.; González, F. J.; Gordillo, B. *J. Electroanal. Chem.* **2003**, *543*, 73.
(37) (a) Kim, H-S.; Chung, T. D.; Kim, H. *J. Electroanal. Chem.* **2001**, *498*, 209. (b) González, F. J.; Aceves, J. M.; Miranda, R.; González, I. *J. Electroanal. Chem.* **1991**, *310*, 293.
(38) (a) Eggins, B. R.; Chambers, J. Q. *J. Electrochem. Soc.* **1970**, *117*, 186. (b) Amatore, C.; Capobianco, G.; Farnia, G.; Sandoná, G.; Savéant, J.-M.; Severin, M. G.; Vianello, E. *J. Am. Chem. Soc.* **1985**, *107*, 1815.
(39) Ortiz, J. L.; Delgado, J.; Baeza, A.; González, I.; Sanabria, R.; Miranda, R. *J. Electroanal. Chem.* **1996**, *411*, 103.
(40) Aguilar-Martínez, M.; Macías-Ruvalcaba, N. A.; Bautista-Martínez, J. A.; Gómez, M.; González, F. J.; González, I. *Curr. Org. Chem.* **2004**, *8*, 1721.
(41) (a) Frontana, C.; Frontana, B.; González, I. *J. Electroanal. Chem.* **2004**, *573*, 307. (b) Frontana, C.; González, I. *J. Braz. Chem. Soc.* **2005**, *16*, 299−307.

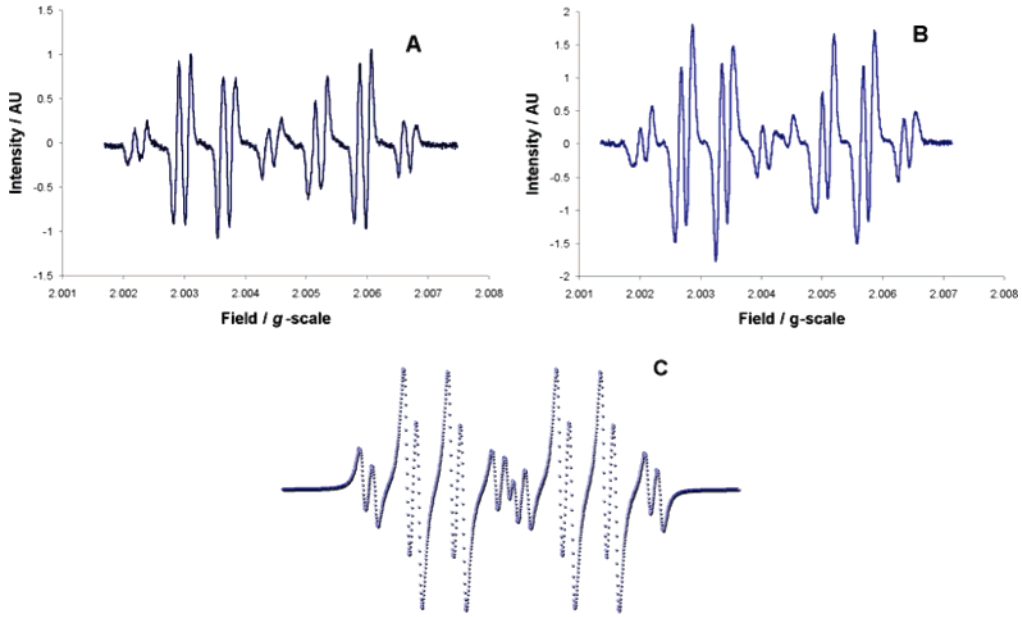

FIGURE 3. ESR spectra of the electrogenerated radical dianions of compounds (A) **1**; (B) **1-H$_2$**, at potential values more negative than the corresponding II_c signals. (C) Simulated spectrum obtained from experimental hyperfine coupling constant (*a*) values.

chemical structure for this last intermediate can be indicative of the changes in chemical environment for both compounds. This is proposed since the analysis in terms of chemical structures for these types of intermediates can be performed with relative ease by employing simultaneous electrochemical−electron spin resonance (EC−ESR) experiments.[41]

II. ESR Behavior of the Radical Dianions for 1 and 1-H$_2$. Figure 3 shows the ESR spectra of the electrogenerated radical dianions of compounds **1** (a) and **1-H$_2$** (b), formed at potential values more negative than the corresponding II_c signal (Figures 1 and 2), while the simulated isotropic structure is depicted in Figure 3C.

The experimental results show that the spectral structure is similar for both radical dianions. However, the corresponding *g* values for compounds **1** and **1-H$_2$** are different: 2.0047 for **1** and 2.0042 for **1-H$_2$**. The latter is closer to the *g* value of an unpaired electron (≈2.0023). This fact indicates that the negative environment caused by the radical dianion structure is more pronounced for **1-H$_2$**. Therefore, it can be considered a more stable conjugated base. This is consistent with the previous experimental report stating that the stability of the electrogenerated hydroquinone for each compound differs in the degree of protonation and is more pronounced for **1-H$_2$**.[41]

From the shape of the spectra depicted in Figure 3, the coupling structure of the electrogenerated semiquinones can be analyzed. These coupling patterns arise from the interaction between the unpaired electron and the H atoms present in the molecule. The values of the hyperfine coupling constants (*a*) can be obtained using simulation procedures. Three main coupling constants were obtained, one for the H atom at the C6 position (doublet), another with the H atoms at the CH_3 group at C7 (quartet), and another with the H atom at the C9 position. The *a* values observed show differences between each compound. These differences are more pronounced for the H atoms at positions C6 and C7 (a_{H-6} = 3.9 [**1**], 4.02 [**1-H$_2$**]; a_{H-7} = 1.26 [**1**], 1.16 [**1-H$_2$**]). In the case of the H atoms at the C9 position, this difference is less significant (a_{H-9} = 0.32 [**1**], 0.30 [**1-H$_2$**]). This indicates that, in the radical dianion structure, the spin density at C6 and C7 changes by the presence or absence of the double bond at positions C12 and C13. However, the magnitude of these changes is very small, which suggests that the observed interaction involves a small energy change between both structures.

These results indicate that, in some way, the double bond located at C12−C13 affects the electronic density in the dianion radical formed in reaction 7. These changes are compatible with those analyzed in terms of the electrochemical study presented in section I. These results are also in good agreement with those reported by the EPR, ENDOR, TRIPLE,[16] EPR spectroelectrochemistry,[18] and recently developed DFT[42] studies of diverse ubiquinones. The results indeed suggest that the double bond at C12−C13 in **1** interacts with the electronic density of the quinone system. It then became necessary to establish the mechanism by which the unsaturation stabilizes and protects **1** against reduction. This mechanism was studied using computational methods.

III. Computational Study of the Electronic Properties of 1 and 1-H$_2$. A computational study of the different conformers generated by the twirl of the carbon−carbon bond in the lateral chain was performed. Since the process corresponds to an intramolecular interaction, there is no basis set superposition error.[26,43] In addition, since dispersion forces may have a relevant role in the process, the MP2 method was selected using in addition a split valence double-ξ basis set with polarization in heavy and light atoms: 6-31G(d,p). The size of this sesquiterpene molecule makes it impossible to include diffuse functions in the basis set used during the optimization procedure. There have been reports of calculations of the Hartree−Fock and DFT hybrid type of folded ubiquinones to explain their low diffusion coefficients and the flexibility.[15−17] The studies were limited to ubiquinone Q_1 due to the limitations associated with the size of the molecules under study. Therefore, the results can only

(42) Kacprazk, S.; Kaupp, M.; MacMillan, F. *J. Am. Chem. Soc.* **2006**, *128*, 5659.

(43) (a) Boys, S. F.; Bernardi, F. *Mol. Phys.* **1970**, *19*, 553. (b) Simon, S.; Duran, M.; Dannenberg, J. J. *J. Chem. Phys.* **1996**, *105*, 11024.

SCHEME 3. Conformers 1a to 1f of Perezone Fully Optimized at MP2/6-31G(d,p) with No Imaginary Frequencies

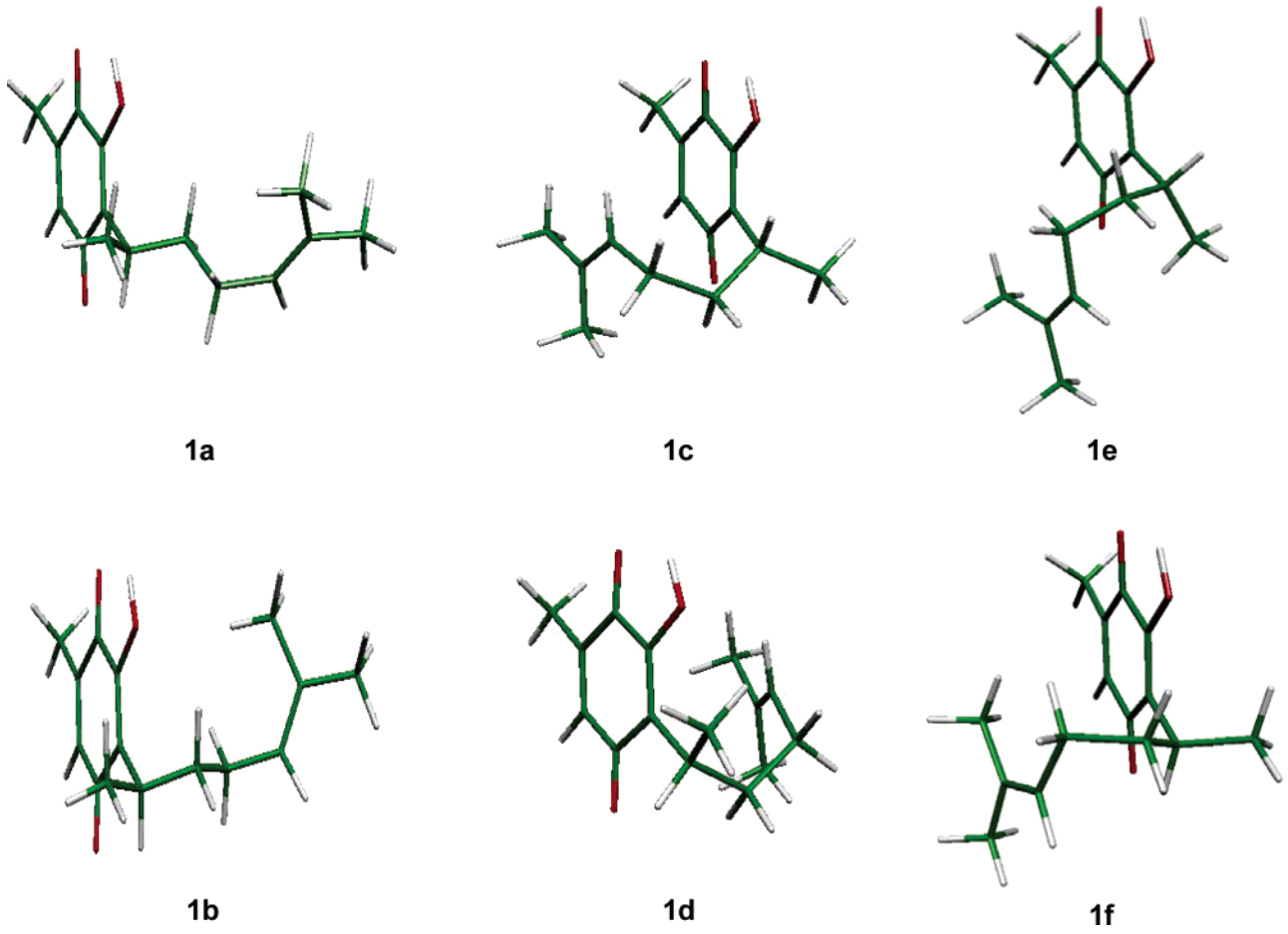

TABLE 1. Relative Energies (kcal/mol) in Relation to Conformer 1a of Perezone and Its Cycloaddition Products at MP2/6-31G(d,p) and MP2/6-31++G(d,p)//MP2/6-31G(d,p) and Its HF Contributions

	1a	1b	1c	1d	1e	1f	α-pipitzol	β-pipitzol
MP2/6-31G(d,p)	0.00	−1.87	−3.71	−0.61	1.44	−4.12	−32.76	−32.57
HF/6-31G(d,p)	0.00	0.29	3.94	6.81	5.90	2.63	−13.67	−12.59
MP2/6-31++G(d,p)	0.00	−2.24	−5.37	−1.90	1.34	−5.60	−32.39	−32.42
HF/6-31++G(d,p)	0.00	0.51	4.86	7.81	6.68	3.55	−11.68	−10.66

show a trend but are not conclusive. In addition, it must be considered that the methods do not include dispersion terms questioning the real participation of these conformers in the equilibrium.

Experimental data were also gathered. The solid-state data of **1** obtained by X-ray diffraction allowed us to establish the conformation in the solid state, in which the segments C2−C9−C10−C11 and C9−C10−C11−C12 adopt the *anti* arrangement.[44] Yu et al. described a similar conformation for the side chain of ubiquinone.[12] However, at the MP2/6-31G(d,p) level, this conformation is not a stationary state, and thus the geometry in the solid-state could be controlled by the crystal packing forces.

The conformer obtained by the full optimization of the quinone with the C2−C9−C10−C11 and C9−C10−C11−C12 segments in an *anti* relation (**1a**, Scheme 3, Tables S1 and S2) was used as reference for this study. This conformer should be the most stable arrangement if only steric arguments are considered. However, conformer **1f** was the most stable by 4.12 kcal/mol (Table 1), followed by conformer **1c** by 3.71 kcal/mol (Scheme 3). In the former conformer, the segments C2−C9−C10−C11 and C9−C10−C11−C12 are maintained in *gauche* disposition with the double bond located over the carbonyl group C1═O of the quinone. On the other hand, the lateral chain of conformer **1c** also adopts consecutive *gauche* arrangements, but it involves the turn of bond C11−C12 with relation to **1f**. Conformer **1c** shows that the double bond adopts a proximal position in relation to the quinone ring. On this conformer, the C7 methyl group and the hydrogen atom in position C6 are closer to methyl C14. This is in contrast to the disposition of substituents in **1f** where they are closer to methyl C15.

Conformer **1d** is only 0.61 kcal/mol more stable than **1a** (Table 1). For **1d**, segments C2−C9−C10−C11 and C9−C10−C11−C12 maintain a *gauche* arrangement similar to that maintained by segment C8−C9−C10−C11. This is in contrast to conformer **1c** where this segment adopts an *anti* arrangement. The approximation of the isopropylidene group to each of the

(44) Soriano-García, M.; Toscano, R. A.; Flores-Valverde, E.; Montoya-Vega, F.; López-Celis, I. *Acta Crystallogr.* **1986**, *C42*, 327.

diastereotopic faces of the quinone ring gives a different disposition to the C8 methyl group of the latter two conformers.

Minimum **1b** shows an *anti* arrangement in the C9−C10−C11−C12 segment but is *gauche* in the C2−C9-C10−C11 segment, provoking a more distant location of the isopropylidene group in relation to the ring. Finally, conformer **1e** is the only one that is less stable than the reference conformer **1a**. Here, the chain has a *gauche* arrangement for the C2−C9−C10−C11 segment but a *gauche* arrangement for segment C9−C10−C11−C12, increasing the distance between the isopropylidene group and the quinoid ring and making any stabilizing effect generated by the interaction of the double bond with the ring impossible.

In butane, where the participation of any additional conformational effect (i.e., *gauche* effect[45]) is not expected, the *anti* conformer is 0.9 kcal/mol more stable than the *gauche* conformer.[46] This gives an indirect idea of the amount of energy compensated by the stabilizing interaction present in these systems. Thus, if the additivity of interactions is accepted, these two *gauche* interactions require at least 1.8 kcal/mol to be surpassed.[46]

From the molecular geometry stand, in conformer **1c**, the distance between C6 and C13 is 3.59 Å and the distance between C2 and C12 is 2.91 Å, while for **1d**, distances are 3.97 and 2.97 Å, respectively. For conformer **1f**, these distances are longer, 3.28 (C2 in relation to C12) and 4.14 Å (C6 in relation to C13), but their stability is not originated in the interaction with the quinone ring. It is generated by the π/π interaction between the olefin and the C1═O carbonyl group. The most relevant distances between the carbonyl group and the double bond of the isopropylidene moiety in conformer **1f** are as follows: C12−C1 2.140 Å, C13−C1 3.250 Å, C12−O1 3.390 Å, and C13−O 3.260 Å.

These results lead one to question the importance of the dispersion forces in the conformational process. In order to determine their importance, we optimized the geometry of stationary states **1c** and **1d** at the B3LYP/6-31G(d,p) level. This level of theory was chosen because this functional includes correlation that does not include dispersion terms. Conformer **1d** is less stable by 3.29 kcal/mol in relation to the conformer of reference **1a**, while conformer **1c** is 1.43 kcal/mol higher in energy. In this conformer, the distance between atoms C6 and C13 is 4.29 Å, and the distance between C2 and C12 is 3.15 Å. In conformer **1d**, they are at 5.21 and 3.33 Å, respectively. More interesting is conformer **1b**, where this hybrid functional describes it as more stable (by 0.46 kcal/mol) than **1a**. This is in agreement with a purely steric explanation of the phenomena.

Since the MP2 method includes the dispersion energies, it predicts more stable conformers and shorter interaction distances. The results showed that supramolecular arrangements calculated with the B3LYP functional include serious problems in the description of the interaction.[26]

Table S3 of the Supporting Information shows the relative stability of the conformers of interest and shows that it is not affected by the inclusion of the zero-point energy. Thus, conformers **1f** and **1c** are the most stable. Conformer **1f** is more stable by 3.87 kcal/mol and **1c** by 3.25 kcal/mol. The scaling factor used for these calculations was 0.96.[47]

Table 1 shows that the inclusion of diffuse functions in the calculation basis set increases the stability of all conformers in relation to **1a**. Even conformer **1e** decreases its energy in relation to **1a**. The trend for all values is preserved in relation to those obtained using the 6-31G(d,p) basis set. In addition, the relative stability order is maintained, showing that the inclusion of diffuse functions does not encourage a substantial change in results. The contribution of Hartree−Fock (HF), presented in Table 1, is very important because all conformers herein studied are substantially less stable than conformer **1a**. Even the loss of stability experienced by conformer **1e** is increased when diffuse functions are included in the calculation basis set. This can be originated by the fact that eliminating the terms that include the dispersion (with a stabilizing contribution) results in a geometry that presents a severe steric repulsion. Thus the minima for HF should occur at a longer distance between the interacting atoms. This is clearly observed in the results that use the B3LYP functional and has been described for other complexes where dispersion is important.[26]

The optimization of the geometry for **1-H$_2$** (see geometry in the Supporting Information) led us to find that the most stable conformer (minimum without imaginary frequencies) is the one where the lateral chain is maintained in an all *anti* conformation. Due to the change of hybridization of segment C12−C13, it is not possible to optimize conformers where the isopropyl group is located in close proximity to the quinone ring. The resulting conformers can be easily explained when the increase in energy that causes the *gauche* in relation to the *anti*[46] arrangement is considered. The minima at MP2/6-31G(d,p) are similar to those obtained at the B3LYP/6-31G(d,p) level.

The thermal treatment of **1** leads to the isolation of a colorless crystal.[48] The study of the reaction led to the conclusion that this compound is actually the mixture of two sesquiterpenes with cedrene skeleton denominated α- and β-pipitzol (Scheme 4). These compounds may be originated from a sigmatropic transposition of an order of [1,9] or from an ionic [5 + 2] cycloaddition reaction[49] from conformers **1c** and **1d**, herein described for the first time. However, it is important to establish if the interaction between the atoms in the quinone ring and those in the double bond in **1c** and **1d** is possible.

The fact that two atoms of a molecule are close in space does not provide enough criteria to establish that there is interaction between them.[50,51] The Atoms in Molecules Theory was used because, within this theory, it possible to rigorously define properties of the electron density. Critical points in addition to the first and second derivatives can be determined with the use of the PROAIM program.[52] According to the AIM theory, the presence of a bond path and its associated virial path provides a universal indicator of bonding[53] or at least interaction between

(45) Juaristi, E.; Cuevas, G. *The Anomeric Effect*; CRC Press: Boca Raton, FL, 1994.

(46) Eliel, E. L.; Wilen, S. H. *Stereochemistry of Organic Compounds*; Wiley-Interscience: New York, 1994; p 600.

(47) (a) Pople, A.; Scott, A. P.; Wong, M. W.; Radom, L. *Isr. J. Chem.* **1993**, *33*, 345. (b) Zhao, Y.; Truhlar, D. G. *J. Phys. Chem. A* **2004**, *108*, 6908. (c) Scott, A. P.; Radom, L. *J. Phys. Chem.* **1996**, *100*, 16502.

(48) Armendáriz, E. *Anales del Instituto Médico Nacional*. Tomo I. Oficina Tipográfica de la Secretaría de Fomento, México, 1894.

(49) Joseph-Nathan, P.; Mendoza, V.; García, E. *Tetrahedron* **1977**, *33*, 1573.

(50) Wiberg, K. B.; Castrejon, H.; Bailey, W. F.; Ochterski, J. *J. Org. Chem.* **2000**, *65*, 1181.

(51) Cortés-Guzmán, F.; Hernández-Trujillo, J.; Cuevas, G. *J. Phys. Chem. A* **2003**, *107*, 9253.

(52) Beigler-König, F. W.; Bader, R. F. W.; Tang, T. H. *J. Comput. Chem.* **1982**, *3*, 317.

SCHEME 4. Structure of α- and *β*-Pipitzol Generated by the Thermal Reaction of Perezone (1)

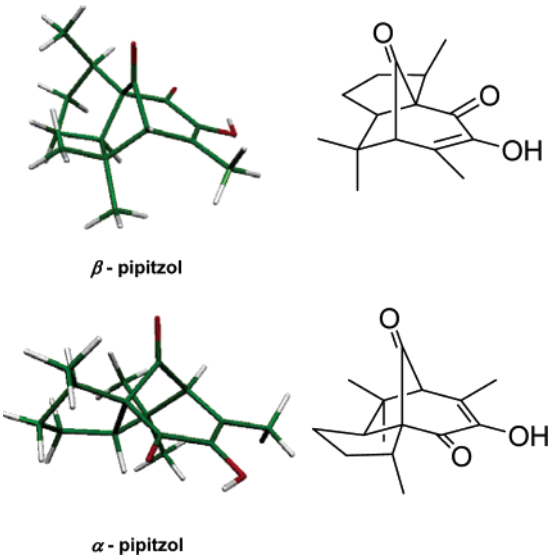

atoms. Since weak interactions are primarily the result of correlation of the electron motions on the two interacting species, their description requires the use of densities obtained from correlated wave functions, determined in a precise manner by the MP2 method. In this way, the analysis of the electronic density of the different perezone conformers should help to establish the existence of an interaction between the olefin, apparently in remote position, and the quinoid ring.

Scheme 5 shows the distribution of critical points in the electronic density of the five key perezone conformers, while Table 2 presents their electronic properties. In conformer **1a**, the bond critical point (*a*) and that of the ring associated with the hydrogen bridge can be observed. The hydroxy group at position 4 participates in the formation of two additional contacts with neighboring hydrogen atoms, analogous to hydrogen bridges of the CH−O type (c and d). The carbonyl group at position C1 forms a hydrogen bridge with atoms at position 9. The observation of the bond critical point of H−H type between one of the hydrogen atoms at position 11 with the methyl at position 14 and its importance in the understanding of the origin of 1,3-*syn*-diaxial repulsion is of interest.[51]

The electron density of a critical point of a weak bond is 20 times less than the density of a critical point in a normal C−H bond. These results agree with those reported by Cioslowski for weak bonds in charge-transfer complexes.[54] The positive value of $\nabla^2\rho$ (ρ) (which is equal to the sum of three curves of ρ) on the critical bond points is related to the interaction of

SCHEME 5. Critical Points in Electronic Density of Some Conformers Related to Perezone (1)

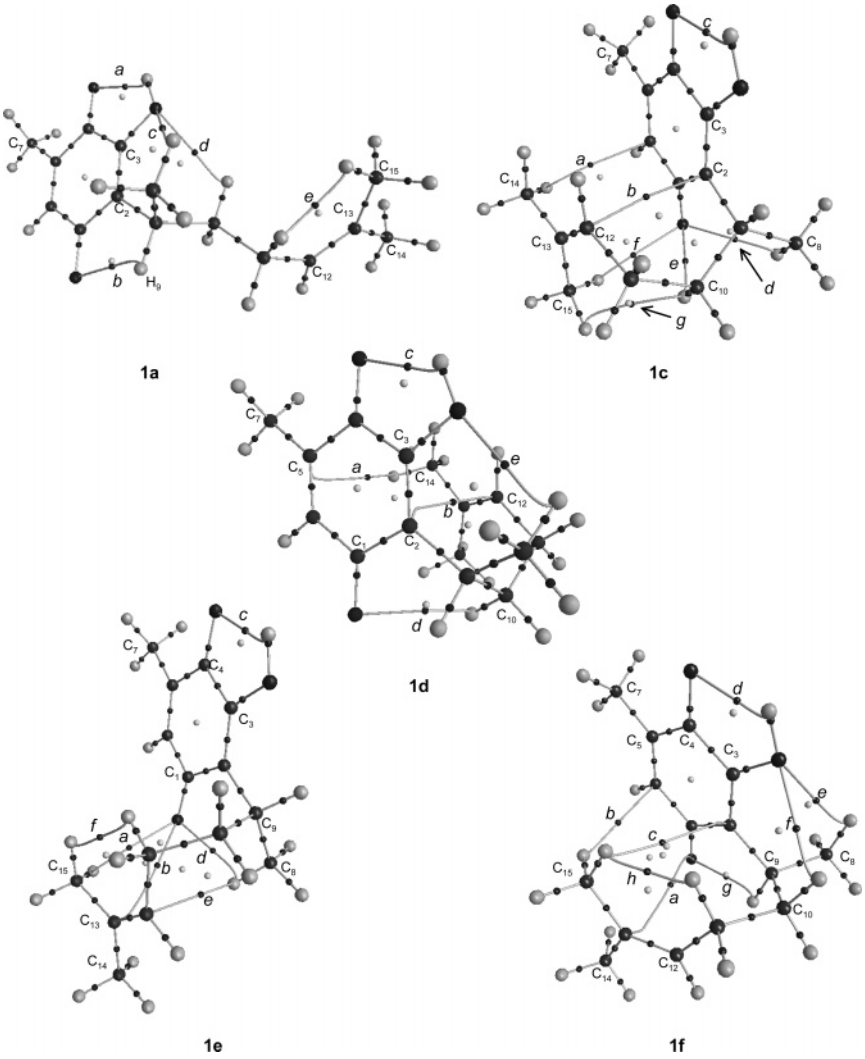

TABLE 2. Critical Point Properties for Relevant Perezone (1) Conformers

point[a]	ρ(e/a$_o^3$)	$\nabla^2\rho$	*e*	*x*[b]	*y*[b]	*z*[b]	TBP[c]	GD[d]
1a:**a**	0.027	0.107	0.408	−0.033	−0.024	0.164	4.016	3.752
1a:**b**	0.016	0.070	1.756	−0.016	−0.006	0.091	4.619	4.403
1a:**c**	0.011	0.041	0.168	−0.010	−0.008	0.059	4.788	4.670
1a:**d**	0.009	0.035	0.227	−0.008	−0.006	0.049	4.930	4.827
1a:**e**	0.012	0.047	0.577	−0.012	−0.007	0.066	4.228	3.905
1c:**a**	0.005	0.017	0.979	−0.003	−0.002	0.022	5.988	5.621
1c:**b**	0.013	0.039	0.163	−0.008	−0.007	0.053	5.550	5.516
1c:**c**	0.026	0.105	0.463	−0.032	−0.022	0.159	4.059	3.780
1c:**d**	0.010	0.038	0.296	−0.009	−0.007	0.054	4.944	4.791
1c:**e**	0.013	0.047	0.175	−0.012	−0.010	0.070	4.676	4.552
1c:**f**	0.007	0.027	0.194	−0.006	−0.005	0.038	5.079	4.985
1c:**g**	0.007	0.029	1.279	−0.004	−0.002	0.034	5.089	4.514
1d:**a**	0.004	0.012	0.376	−0.003	−0.002	0.017	6.893	6.040
1d:**b**	0.013	0.038	0.570	−0.008	−0.005	0.051	5.904	5.617
1d:**c**	0.029	0.113	0.332	−0.036	−0.027	0.176	3.912	3.690
1d:**d**	0.010	0.039	0.473	−0.008	−0.005	0.052	4.993	4.811
1d:**e**	0.013	0.054	0.565	−0.012	−0.007	0.073	4.944	4.584
1e:**a**	0.008	0.032	0.763	−0.006	−0.003	0.041	5.501	5.021
1e:**b**	0.006	0.022	2.100	−0.004	−0.001	0.027	6.802	6.186
1e:**c**	0.026	0.106	0.451	−0.032	−0.022	0.160	4.053	3.774
1e:**d**	0.014	0.056	0.353	−0.014	−0.010	0.081	4.765	4.505
1e:**e**	0.010	0.033	0.239	−0.008	−0.007	0.048	4.983	4.876
1e:**f**	0.012	0.046	0.458	−0.012	−0.008	0.066	4.125	3.877
1f:**a**	0.006	0.019	2.147	−0.002	−0.001	0.022	7.038	6.397
1f:**b**	0.006	0.020	0.214	−0.004	−0.003	0.028	5.436	5.322
1f:**c**	0.005	0.015	1.041	−0.002	−0.001	0.018	6.322	6.004
1f:**d**	0.026	0.106	0.422	−0.033	−0.023	0.162	4.030	3.761
1f:**e**	0.007	0.029	1.072	−0.005	−0.002	0.036	5.293	5.103
1f:**f**	0.011	0.043	0.236	−0.010	−0.008	0.061	4.852	4.679
1f:**g**	0.016	0.071	4.224	−0.015	−0.003	0.089	4.692	4.424
1f:**h**	0.012	0.047	0.402	−0.013	−0.009	0.070	4.024	3.806

[a] See figures for numbering. [b] Eigenvalues of the Hessian at critical points. [c] Total bond path (au). [d] Geometric distance (au).

closed shell systems, ionic bonds, hydrogen bonds, and van der Waals bonds, to which a notable ionic character may be assigned,[55] but are of attractive nature.

Conformer **1c** shows a bond trajectory between C2 and C12 (point b) that corresponds with the incipient formation of the C−C bond that will originate the pipitzol during the thermal rearrangement. Due to the angular compression caused by the approximation of the olefin to the quinone, which produces a five-membered ring, the second carbon atom of the olefin cannot approach to a position where a second C−C interaction can occur. Thus, a hydrogen atom of the terminal methyl group stabilizes the structure (point a on conformer **1c**, Scheme 5). Similar interactions are observed in conformer **1d**. Table 1 and Scheme 4 present information on the aforementioned pipitzols. Undoubtedly, conformers **1c** and **1d** correspond to the intermediaries in the cycloaddition process that forms α- and *β*-pipitzols.

Conformers **1e** and **1f**, in addition to presenting interactions similar to those previously described (hydrogen bridges and H−H contacts), are characterized by the existence of interactions between the carbons that form the C═C double bond of the isopropylidene group and the carbonyl group. The ring interactions (interactions **1e**:**b** and **1f**:**a**) are not present. This shows that the interactions present in the system are evident through the stabilization observed through the relative energies shown in Table 1.

From the kinetic point of view, the formation of five- or six-membered rings is favored in comparison to larger rings. The approximation of the lateral chain over the quinoid ring leads to stationary states that resemble precisely five- or six-membered rings, so the interaction with the first or second isoprene

SCHEME 6. Critical Points in Electronic Density of Some Relevant Conformers of Homoperezone (5)

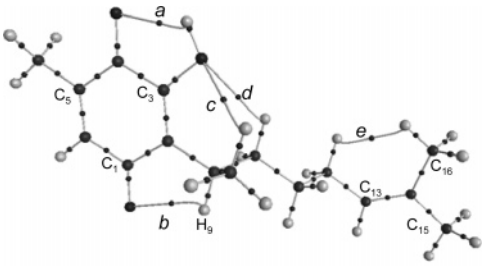

5a

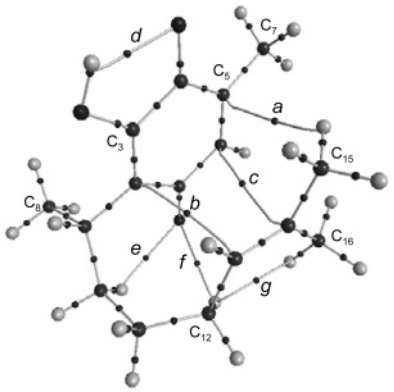

5c

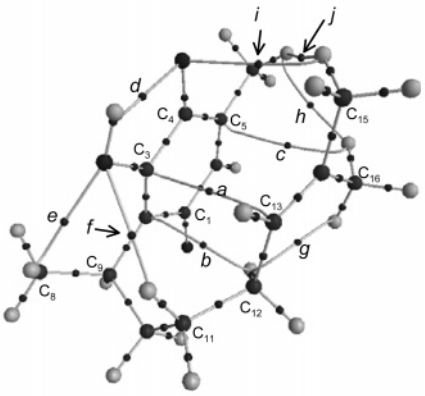

5d

fragment in the ubiquinone series should be favored just as it has been demonstrated.[13] On the other hand, the difference in energy between conformers **1c** and **1d** could be due to the *gauche* arrangement of the methyl group in the $C_8-C_9-C_{10}-C_{11}$ segment experienced by the less stable conformer.

In principle, the addition of an extra methylene group to the lateral chain can decrease the angular requirements that are hindered by the approximation of the lateral chain to the quinoid ring of perezone.

Calculations at the same levels of theory were also performed for homoperezone (**5**, Scheme 1). Results are shown in Scheme 6 and Table 3. The extended conformer (**5a**) has an energy of −846.03461 Hartrees. Conformer **5c** that generates the *β*-isomer of homopipitzol is 1.44 kcal/mol more stable, while **5d**, which could generate α-homopipitzol, is only 0.18 kcal/mol less stable than **5a**. The inclusion of diffuse functions increases the stabilizing effects similar to that observed in conformers of **1**; nevertheless, the HF energy calculated with MP2 geometry

SCHEME 7. Comparative NOE Effective of 1-H_2 (left) and 1 (right) That Shows the Proximity of the Propenyl Group and the Methyl Group at Position 7 of Compound 1

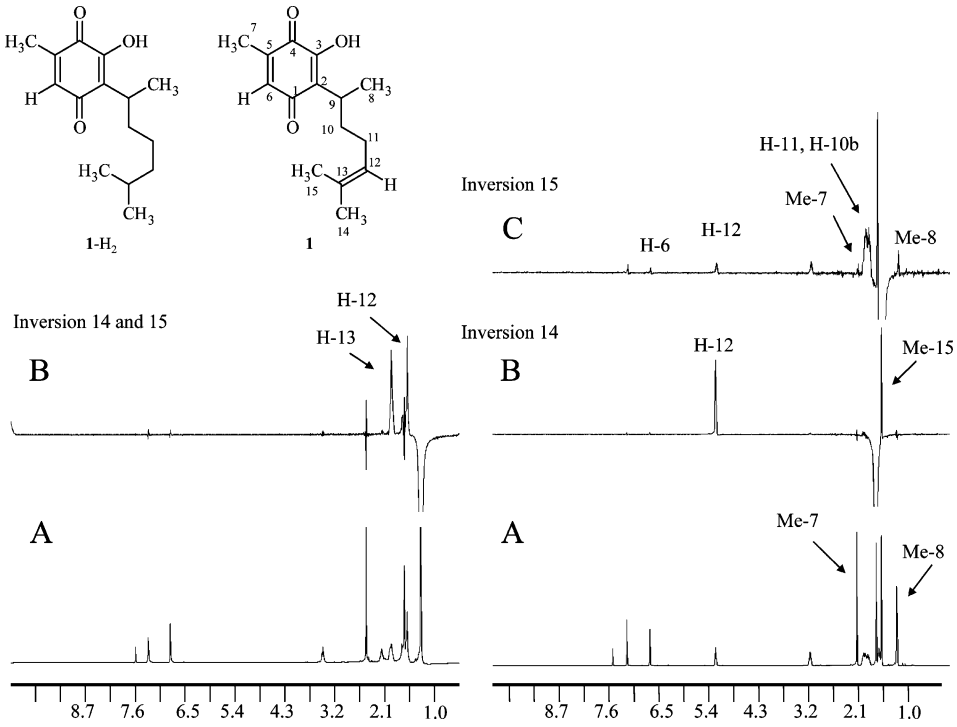

TABLE 3. Total Energy (Hartrees) and Differences (kcal/mol) of the Conformers of Homoperezone 5 at MP2/6-31G(d,p), HF/6-31G(d,p)//MP2/6-31G(d,p), MP2/6-31++G(d,p)//MP2/6-31G(d,p), and HF/6-31++G(d,p)//MP2/6-31G(d,p)

		E_{MP2}	E_{rel}[a]	E_{HF}	E_{rel}[a]
6-31G(d,p)	**5a**	−846.03461	0.00	−843.29359	0.00
	5c	−846.03690	−1.44	−843.27703	10.39
	5d	−846.03490	−0.18	−843.27503	11.65
6-31++G(d,p)	**5a**	−846.08485	0.00	−843.31183	0.00
	5c	−846.09043	−3.50	−843.29341	11.56
	5d	−846.08815	−2.07	−843.29126	12.91

[a] Relative energies with respect to homoperezone **5** at its conformation **5a**.

shows a severe repulsion since the terms that produce stabilization are not included at this level.

The properties of the critical points of conformers **5a** and **5c** and their distribution are analogous to that of perezone conformers **1a** and **1c**. However, conformer **5c** shows a substantial difference in relation to **1c** since there are the two expected C−C bond trajectories between the olefin and quinone carbon atoms, as is expected in terms of homopipitzol formation (see Table S4 in the Supporting Information).

IV. NMR Evidence of the Existence of Conformers 1c, 1d, and 1f. In reality, the question regarding the nature of conformers **1c**, **1d**, and **1f** is raised. Is it possible that these are real, or are they a mere product of performing calculations in gas phase at 0 K? It was still necessary to investigate if conformers **1c**, **1d**, and **1f** really take part in the conformational population of perezone. To determine this, a nuclear magnetic resonance (NMR) study of the compound in a deuterated chloroform solution was conducted (Scheme 7).

The characteristic signals of **1** were easily assigned (Scheme S1). NOE experiments were performed to detect the possibility of close proximity between the quinone ring and the lateral chain in **1**. Since the proximity could be simply due to a nonspecific process generated by the turning of the lateral chain when passing over the quinone ring, the hydrogenated derivative was also studied (**1-H_2**).

For both compounds (Scheme 7), the methyl groups at positions 14 and 15 were inverted with a 180 selective pulse, and the corresponding NOEs were monitored after mixing periods of 600 and 900 ms, in both cases.

The different behavior for both compounds is notorious. In **1**, small but detectable NOEs (Scheme 7) were observed for H-6 (0.6−0.8%) and Me-7 (0.4−0.5%) in the quinone ring, upon inversion of Me-15, besides the trivial NOEs to H-9, H-10, and H-11. In contrast, no NOE was detected for the same protons (H-6, Me-7) attached to the quinone ring for compound **1-H_2**. In this case, the overlapping between both methyl groups 15 and 14 allowed their simultaneous inversion. Only NOEs to the other side chain protons were observed. This indicates that the C12−C13 double bond is required for establishing the observed side chain−quinone ring interaction in **1**, and that the residence time of the olefin over the quinone is long enough to allow the transfer of information between the atoms in the proximity. It would be expected that conformer **1f** would be mainly responsible for this behavior because, in this conformer, the irradiated methyl C15 is close to methyl C7 and the hydrogen atom in position C6. Although this conformer is more stable (according to the calculations) and interacts with the carbonyl group, it

(53) (a) Bader, R. F. W. *J. Phys. Chem. A* **1998**, *102*, 7314. (b) Bader, R. F. W.; Carroll, M. T.; Cheesman, J. R.; Chang, C. *J. Am. Chem. Soc.* **1987**, *109*, 7968. (c) Bader, R. F. W. *Atoms in Molecules: A Quantum Theory*; Clarendon Press: Oxford, 1990. (d) Bader, R. F. W. *Chem. Rev.* **1991**, *91*, 893.

(54) (a) Cioslowski, J.; Mixon, S. T. *J. Am. Chem. Soc.* **1992**, *114*, 4382. (b) Cioslowski, J.; Mixon, S. T.; Edwards, W. D. *J. Am. Chem. Soc.* **1991**, *113*, 1083.

(55) (a) Kremer, D.; Kraka, E. *Croat. Chem. Acta* **1984**, *57*, 1265. (b) Bader, R. F. W.; Tal, Y.; Anderson, S. G.; Nguyen-Dang, T. *Isr. J. Chem.* **1989**, *19*, 3234.

does not produce pipitzols. However, when the hydrogen atoms of the methyl groups C7 or C6 are inverted, it is possible to observe the NOE for both methyl C15 and C14 (Scheme S3). This supports the real existence of conformers **1c** and **1d**.

These interactions may also explain the decrease of the diffusional current for **1-H$_2$** compared to that for **1**. This can be explained considering that **1** adopts a more compact geometry due to the interaction of the double bond at positions C12−C13 with the quinone ring, and consequently, **1** has a higher diffusion coefficient than **1-H$_2$**, which adopts a more extended geometry as it lacks this interaction. This results in a minor diffusion coefficient supporting what was previously proposed in this study. Thus, the existence of conformers **1c** and **1d**, due to the π/π interaction, can be demonstrated.

The volume inside a contour of 0.001 electrons/bohr^3 was calculated for conformers **1a**, **1b**, **1c**, and **1d**. At B3LYP/6-31G(d,p), values are 209.3, 215.3, 177.5, and 183.8 cm^3/mol, respectively. Similar values at the MP2/6-31G(d,p) level were obtained: 229.5, 203.2, 179.8, and 197.3 cm^3/mol, respectively, in perfect agreement with expectations. Extended conformers have larger volumes.

On the other hand, the UV−visible spectra of **1** and **1-H$_2$** showed small but noticeable differences that become important in light of the results described. Compound **1** in methanol presents maxima at 410, 266, and 204 cm^{-1} and minima at 326 and 237 cm^{-1}, while **1-H$_2$** presents maxima at 408, 266, and 205 and minima at 318 and 235 cm^{-1}. These results can also be explained by considering the presence of a small concentration of the conformers where the olefin of the isopropylidene group is close to the quinoid ring of **1**.

Conclusions

This study shows the importance of weak interactions of olefin quinone type in the reduction process of quinones. These interactions can protect the molecules in biological media or at least modulate their electrochemical potential modifying the conformation. Therefore, these molecules can be activated by only very specific metabolic conditions due to the capability of certain enzymes to recognize diverse conformers.[56] Cyclic voltammetry experiments and coupled electrochemical−electron spin resonance studies showed changes in the reactivity between compounds **1** and **1-H$_2$**. These results are compatible with the presence of a low-energy $\pi-\pi$ interaction between the double bond C12−C13 and the quinone ring. This was also confirmed using computational methods and NMR.

These results show that, in agreement with previously published results,[12] chain flexibility is important for quinone **1** redox properties since it allows the approach of the donating propenyl group to the quinone ring. However, the chain flexibility in itself does not guarantee changes in reactivity. The $\pi-\pi$ interactions between the quinone and the isopropylidene group are the real origin of the change in electrochemical properties that lead to the change in reactivity and conformation. NOE experiments provided experimental data to support the proximity of these groups in stable conformers. Calculations at the MP2/6-31G(d,p) level confirmed that conformer **1a** coexists in solution with other conformers, with at least one *gauche* arrangement in the lateral chain, **1c**, **1d**, or **1f**, that explains the high diffusion coefficients of coenzyme Q$_{10}$.[15] Dispersion forces are responsible for the formation of these arrangements. This study demonstrates the existence of conformers stabilized by $\pi-\pi$ interactions that generate α- and β-pipitzol. This is extremely important because it gives the basis to study similar conformers that must be involved in other cycloaddition processes, such as Diels−Alder reactions. From the biological point of view, the participation of **1** in electron-transfer processes depending on the type of conformer that is recognized by the enzymatic system is of particular relevance and warrants further study in this area.

Experimental Section

Isolation and Hydrogenation of Perezone (1). Perezone was isolated using the procedure reported by Walls et al.[30,31] obtaining golden-yellow leaflets, mp 104−106 °C; $[\alpha]^{20}_D$ −17 (Et_2O).

The reduction with hydrogen over palladium was performed using the method described by Kölg and Boer:[32] IR (KBr, cm^{-1}) 3328, 2925, 2871, 2474, 1643, 1621, 1462, 1378, 1296, 1199, 1116, 1050, 982, 891, 816, 714, 645, 592, 498; UV−vis (MeOH, nm) 408, 318, 266, 235, 205; ^{1}H NMR ($CDCl_3$) δ 0.82 (d, 3H, J = 5 Hz, H15), 0.83 (d, 3H, J = 5 Hz, H14), 1.16 (m, 4H, H11,12), 1.20 (d, 3H, J = 7.0 Hz, H8), 1.51 (m, 2H, H10, H13), 1.72 (m, 1H, H10), 2.06 (d, 3H, J = 1.5 Hz, H7), 3.04 (m, 1H, H9), 6.48 (q, 1H, J = 1.5 Hz, H6), 7.02 (br s, 1H, OH); ^{13}C NMR ($CDCl_3$) δ 187.4 (C1), 184.4 (C4), 150.9 (C3), 140.5 (C5), 135.8 (C6), 124.8 (C2), 38.9 (C12), 34.3 (C10), 29.5 (C9), 27.8 (C13), 25.8 (C11), 22.6 (C14, C15), 22.5 (C15, C14), 18.1 (C8), 14.8 (C7); MS *m*/*z* 250, 235, 167.1, 166.1, 153.1, 137, 109, 43.

Electrochemical Procedure. Solvent and Supporting Electrolyte: Acetonitrile (AN) was dried overnight with $CaCl_2$ and purified by distillation on P_2O_5. Traces of water in the solvent were eliminated by contact with 3 Å molecular sieves in the dark. The absence of the characteristic −OH bands in the IR spectra confirmed the complete elimination of water traces. Tetraethylammonium tetrafluoroborate was dried under vacuum at 60 °C for 8 h before use.

Electrodes, Apparatus, and Instrumentation: Cyclic voltammetry measurements were carried out in a conventional three-electrode cell. A polished glassy carbon electrode (7 mm^2) was used as a working electrode. Before measurements, this electrode was cleaned and polished with 0.05 μm alumina, wiped with a tissue, and sonicated in distilled water for 2−4 min. A platinum wire served as counter electrode. The reference electrode was an aqueous AgCl/Ag electrode immersed in AN for 30 min before use. Peak potentials were measured at controlled temperature (25 °C) in AN solutions using 0.1 M Et_4NBF_4 as the supporting electrolyte. Solutions of 1 mM of **1** and **1-H$_2$** in the electrolytic media were used. At lower concentrations of the electroactive species, the capacitive currents precluded acceptable evaluation of current peaks. Voltammetric curves were recorded using an electrochemical analyzer interfaced with a personal computer. Measurements were made over a potential range between 0.25 and −2.5 V with a scan rates of 0.05−9.0 V·s^{-1}. Before the experiments, sample solutions were purged with nitrogen, which was presaturated with the appropriate solvent containing 3 Å sieves. All potentials were determined under the same conditions to obtain a consistent data set. In order to establish a reference system with the experimental conditions of our particular system, the redox potentials reported in this paper refer to the Fc^+/Fc pair, as recommended by IUPAC.[57] In this case, the potential for the Fc^+/Fc redox pair, determined by voltamperometric studies, was 0.412 V versus SCE.

Electrochemical ESR coupled experiments were obtained using a BAS-100W interfaced with a personal computer. Measurements

(56) (a) Heightman, T. D.; Vasella, A. T. *Angew. Chem., Int. Ed.* **1999**, *38*, 750. (b) García-Herrero, A.; Montero, E.; Muñoz, J. L.; Espinoza, F.; Vian, A.; García, J. L.; Asensio, J. L.; Cañada, F. J.; Jiménez-Barbero, J. *J. Am. Chem. Soc.* **2002**, *124*, 4804.

(57) Gritzner, G.; Küta, J. *Pure Appl. Chem.* **1984**, *56*, 461.

were performed employing a scan rate of 10 $mV \cdot s^{-1}$ and holding the potential scan at a position at which a stable radical signal was recorded on the ESR spectrometer (−1.8 V for **1** and −1.7 V vs Fc^+/Fc for **1-H$_2$**). A commercially available flat path electrochemical cell was employed, using a platinum wire as working electrode (3.1 cm^2) and another platinum wire as counter electrode, separated from the medium by a membrane. Ag/0.01 M $AgNO_3$/0.1 M TBAP in AN was employed as reference electrode. This electrode was referenced to the Fc^+/Fc couple according to the recommendation by the IUPAC in order to maintain comparative conditions with those used for cyclic voltammetry.[57]

ESR spectra were recorded using a ESR spectrometer at X-band (9.72 GHz), employing a rectangular TE_{011} cavity. The modulation amplitude was set at a value low enough to allow a good determination of the hyperfine coupling constant values with a good signal-to-noise ratio.

ESR Simulations. PEST WinSim[58] free software Version 0.96 (National Institute of Environmental Health Sciences) was used to perform simulation of the ESR experimental spectra from the measured hyperfine coupling constant values (*a*). This program was also useful to evaluate *a* values when a direct measurement was difficult in the conditions where the spectra acquisition was performed.

NMR experiments were recorded on a 500 MHz spectrometer, using an approximately 10 mg/mL solution of both compounds at 303 K. One-dimensional NOESY experiments were done using the double pulse field gradient spin echo method[59] with mixing times of 600 and 900 ms.

Theoretical Calculations. Full geometry optimizations (no symmetry constraints) of all compounds were performed at MP2/6-31G(d,p) using the hybrid functional B3LYP with the same basis set. The 6d and 10f orbital functions were used for all compounds. Single-point calculations were performed at MP2/6-31++G(d,p) using the calculated MP2/6-31G(d,p) geometry. These calculations were carried out with the Gaussian 03 program.[60] AIM analyses were performed with PROAIMV.[52]

Acknowledgment. This paper is dedicated to the memory of Dr. Leopoldo Rio de la Loza who isolated perezone for the first time in 1856, in celebration of 200 years of his birth. We are grateful to the reviewers for their useful comments that led to the improvement of this paper. The authors are grateful to the Dirección General de Servicios de Cómputo Académico, Universidad Nacional Autónoma de México DGSCA, UNAM, to Consejo Nacional de Ciencia y Tecnología (CONACYT) for financial support via Grants 49921-Q and 40702-Q, to Dirección General de Asuntos del Personal Académico (DGAPA) via Grant Nos. IN-7200 and IN209606. G.R.-P. and C.F. are grateful to CONACYT-Mexico for the scholarship granted. We are grateful to Rebeca López-García for the revision of the English version of the manuscript.

Supporting Information Available: Cartesian coordinates and energy (Hartrees) of conformers of perezone, α- and *β*-pipitzols, dihydroperezone, and conformers of homoperezone at MP2/6-31G(d,p). Table S1. Energy (Hartrees) at MP2/6-31G(d,p) and HF/6-31G(d,p)//MP2/6-31G(d,p) of the conformers and cycloaddition products of perezone **1**. Table S2. Energy (Hartrees) at MP2/6-31++G(d,p)//MP2/6-31G(d,p), and HF/6-31++G(d,p)//MP2/6-31G(d,p) of the conformers and cycloaddition products of perezone **1**. Table S3. Calculated total energies and zero-point energies (Hartrees) based on optimized full geometries at MP2/6-31G(d,p) of some stationary points of perezone (**1**). Table S4. Critical point properties for the relevant homoperezone (**5**) conformers. Scheme S1. NOE effects of perezone **1**: (a) inversion of proton at C6; (b) inversion of methyl C7. This material is available free of charge via Internet at http://pubs.acs.org.

JO061576V

(58) http://epr.niehs.nih.gov/ pest_mans/winsim.html.

(59) Stott, K.; Stonehouse, J.; Keeler, J.; Hwang T.-L.; Shaka, A. J. *J. Am. Chem. Soc*. **1995**, *117*, 4199.

(60) Frisch, M. J.; Trucks, G. W.; Schlegel, H. B.; Scuseria, G. E.; Robb, M. A.; Cheeseman, J. R.; Montgomery, J. A., Jr.; Vreven, T.; Kudin, K. N.; Burant, J. C.; Millam, J. M.; Iyengar, S. S.; Tomasi, J.; Barone, V.; Mennucci, B.; Cossi, M.; Scalmani, G.; Rega, N.; Petersson, G. A.; Nakatsuji, H.; Hada, M.; Ehara, M.; Toyota, K.; Fukuda, R.; Hasegawa, J.; Ishida, M.; Nakajima, T.; Honda, Y.; Kitao, O.; Nakai, H.; Klene, M.; Li, X.; Knox, J. E.; Hratchian, H. P.; Cross, J. B.; Bakken, V.; Adamo, C.; Jaramillo, J.; Gomperts, R.; Stratmann, R. E.; Yazyev, O.; Austin, A. J.; Cammi, R.; Pomelli, C.; Ochterski, J. W.; Ayala, P. Y.; Morokuma, K.; Voth, G. A.; Salvador, P.; Dannenberg, J. J.; Zakrzewski, V. G.; Dapprich, S.; Daniels, A. D.; Strain, M. C.; Farkas, O.; Malick, D. K.; Rabuck, A. D.; Raghavachari, K.; Foresman, J. B.; Ortiz, J. V.; Cui, Q.; Baboul, A. G.; Clifford, S.; Cioslowski, J.; Stefanov, B. B.; Liu, G.; Liashenko, A.; Piskorz, P.; Komaromi, I.; Martin, R. L.; Fox, D. J.; Keith, T.; Al-Laham, M. A.; Peng, C. Y.; Nanayakkara, A.; Challacombe, M.; Gill, P. M. W.; Johnson, B.; Chen, W.; Wong, M. W.; Gonzalez, C.; Pople, J. A. *Gaussian 03*, revision C.02, Gaussian Inc.; Wallingford CT, 2004.